Available online at www.sciencedirect.com
ScienceDirect
Journal of Nuclear Materials 366 (2007) 297–305
journal of nuclear materials
www.elsevier.com/locate/jnucmat

Kinetics of precipitation of U_4O_9 from hyperstoichiometric UO_{2+x}

J.D. Higgs [a], W.T. Thompson [a,*], B.J. Lewis [a], S.C. Vogel [b]

[a] Department of Chemistry and Chemical Engineering, Royal Military College of Canada, P.O. Box 17000 STN FORCES, Kingston, ON, Canada K7K 7B4

[b] Los Alamos Neutron Science Center (LANSCE), Manual Lujan Jr. Neutron Scattering Center (LANSCE-12), Los Alamos National Laboratory, Mail Stop H805, Los Alamos, NM 87545, USA

Abstract

For safe and reliable operation of fission reactors in space, the phase diagrams and reaction kinetics of systems used as nuclear fuels, such as U–O, U–N, U–C, are required. Diffraction allows identification of phases and their weight fractions as a function of temperature in situ, with a time resolution of the order of minutes. In this paper, we will provide results from a neutron diffraction experiment studying the U–O system. Using the neutron diffractometer HIPPO, the decomposition of UO_{2+x} into UO_2 and U_4O_9 as a function of temperature was investigated in situ. From the diffraction data, the participating phases could be identified as UO_{2+x}, UO_2 and $U_4O_{8.94}$ and no stoichiometric U_4O_9 was found. Results of the experiment were used to improve existing thermodynamic models. The presented techniques (i.e., neutron diffraction and thermodynamic modeling) are also applicable to the other systems mentioned above.

PACS: 61.12.−q; 89.30.Gg; 64.75.+g; 81.05.Je

1. Introduction

Uranium-based fuels have been used for space reactor applications for many years. In particular, uranium dioxide (UO_2) has played an important role as fuel for the TOPAZ space reactors. Therefore, a sound understanding of the U–O system is required for the design, operation and disposal of reactor fuels for space applications.

Oxidation of UO_2 (due to a reaction with air or steam, for example) may result in the formation of higher oxides, such as U_4O_9, U_3O_7 and U_3O_8 [1] depending on the temperature and oxygen partial pressure. The change in density, crystal structure and chemical behaviour accompanying the introduction of these higher phases may have adverse effects on the mechanical and chemical performance of the fuel. Therefore, it is important to understand the stability of the various phases present.

Many investigators have studied the U–O system, most recently summarized by Guéneau et al. [2], Chevalier et al. [3] and Lewis et al. [4] as

* Corresponding author. Tel.: +1 613 541 6000x6081; fax: +1 613 542 9489.
E-mail address: thompson-w@rmc.ca (W.T. Thompson).

0022-3115/$ - see front matter © 2007 Elsevier B.V. All rights reserved.
doi:10.1016/j.jnucmat.2007.03.054

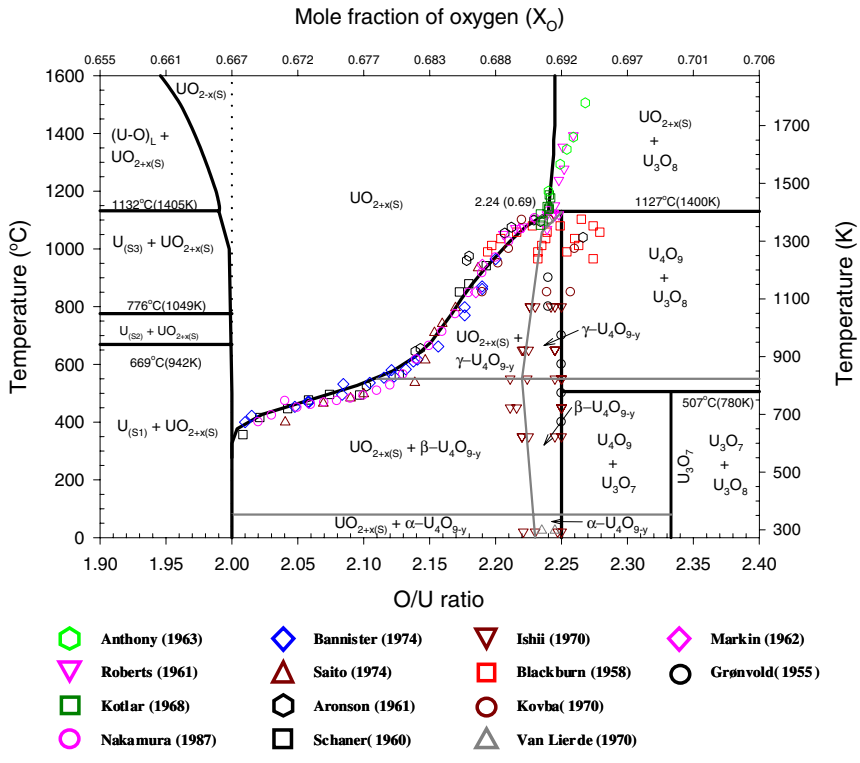

*The horizontal line constructions (grey) at 80°C and 550°C reflect the inability to distinguish the transformation temperatures in the adjacent two-phase fields.

Fig. 1. Calculated U–O phase diagram in area of interest compared with experimental data [6–19] and current treatment of the system [20].

UO_2 has traditionally been a popular fuel for both military and commercial water-cooled power reactors. Therefore, the U–O phase diagram is fairly well established. There still exists, however, some uncertainty around the non-stoichiometry of U_4O_9. Recent attempts to model the U–O system [3] approximate U_4O_9 as stoichiometric. Many investigators, however, have shown that U_4O_9 is a narrowly non-stoichiometric phase (U_4O_{9-y}). Experiments have shown that three phases exist: α-U_4O_{9-y} (below ~80 °C), β-U_4O_{9-y} (between ~80 °C and ~550 °C) and γ-U_4O_{9-y} (above ~550 °C) [5]. Fig. 1 shows a summary of the experimental data [6–19] on the location of the phase boundaries for U_4O_{9-y} as well as the proposed fields for the three phases of U_4O_{9-y} overlaid on the current thermodynamic treatment for this system [20]. In addition, the kinetics of precipitation of U_4O_9 from UO_{2+x} are not well known, only that quenching of UO_{2+x} is required to prevent the formation of U_4O_9 [6,19].

2. Description of experiment

To investigate the non-stoichiometry in U_4O_9 and the kinetics of precipitation of U_4O_9 from UO_{2+x}, an in situ neutron diffraction experiment was performed using the high-pressure preferred orientation (HIPPO) neutron diffractometer [21,22] at the Los Alamos Neutron Science Center (Los Alamos National Laboratory, New Mexico).

The reason neutron diffraction is used instead of X-ray diffraction (XRD) for the study of the U–O system is due to the much deeper penetrating depth into UO_2 with neutrons than with X-rays, so that the results are more representative of the bulk sample. Also, in situ heating of the sample for high temperature studies is more difficult with XRD (i.e., for neutron diffraction the furnace can be designed with materials that are mostly transparent to neutrons). The thermal neutron flux levels of the order of 10^7 n cm^{-2} s^{-1} and detector coverage on the HIPPO instrument are high enough to provide

rapid collection of data but not so high as to induce appreciable neutron capture in the material.

The sample was 6.22 g of depleted UO_{2+x} powder, with x measured to be 0.197 by oxidation in a thermo-gravimetric analyzer (TGA). The sample was loaded in a silica tube and heated from room temperature to a maximum of 1150 °C while exposed to a neutron beam inside the HIPPO neutron diffraction instrument. The temperature of the sample was cycled as shown in Fig. 2. Neutron diffraction data were taken every 10 min (i.e., each run was 10 min in length), allowing quantitative phase analysis with this time resolution. The entire experiment was approximately 24 h in length. A selection of the patterns collected is shown in Fig. 3.

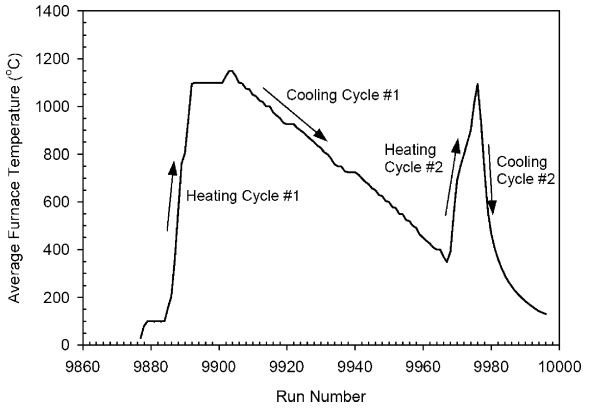

Fig. 2. Cycling of sample temperature.

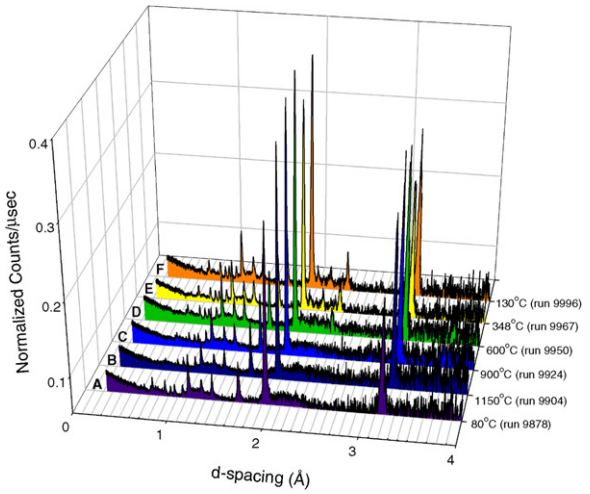

Fig. 3. Diffraction patterns at various points in the experiment, for one of the 90° banks normalized by incident beam count intensity.

3. Data analysis

Rietveld refinement [23] of the diffraction patterns was performed using the General Structure Analysis System (GSAS) software [24]. Diffuse scattering parameters were included to account for the silica glass liner (container). The crystal structures used in the refinement were stoichiometric UO_2 space group Fm3m from Hutchings [25] and $UO_{2.234}$ space group $I\bar{4}3d$ from Kim et al. [26]. The observed patterns also matched the $I\bar{4}3d$ structure reported by Copper and Wills [27]. Many other crystal structures reported were tried, such as U_4O_9 space group $I4_132$ from Masaki and Doi [28], and U_4O_9 space group $I\bar{4}3d$ from Belbboch et al. [29]. Only the $UO_{2.234}$ space group $I\bar{4}3d$ structure produces the peaks around a d-spacing of 2.3 Å as seen in the diffraction patterns and thus only this crystal structure could fit the patterns for peaks generated from a U_4O_9 (or more precisely a U_4O_{9-y}) phase.

The $UO_{2.234}$ phase could also be considered $U_4O_{8.936}$, or U_4O_{9-y}, where y is 0.064. The excellent fit to the U_4O_{9-y} phase ($UO_{2.234}$), as well as the fact that the data did not fit any published patterns of stoichiometric U_4O_9, is further evidence that U_4O_9 does indeed have a non-stoichiometric field.

Rietveld refinement of the diffraction patterns provided a measure of the respective lattice parameter and weight fraction for each phase present in the sample at many sample temperatures (see Fig. 4). Refined UO_2 weight fractions from the refinement are shown in Fig. 5 and refined lattice parameters for each phase are shown in Figs. 6 and 7.

4. Discussion of results

One result from this experiment of particular interest is the weight fraction of UO_2 at the beginning of the experiment (Fig. 5) and its accompanying lattice parameter (Fig. 6). On the initial heat up of the sample, the UO_2 phase weight fraction is much higher (~100% instead of ~30%) and its lattice constant is lower than would be expected from the phase diagram and published lattice parameter data for stoichiometric UO_2 (this can also visually seen from the patterns in Fig. 3). These results would suggest the sample was initially a metastable single phase of UO_{2+x}. It is surmised that the additional thermal energy added to the sample on initial heating was sufficient to precipitate U_4O_{9-y} from UO_{2+x}, bringing it into thermodynamic equilib-

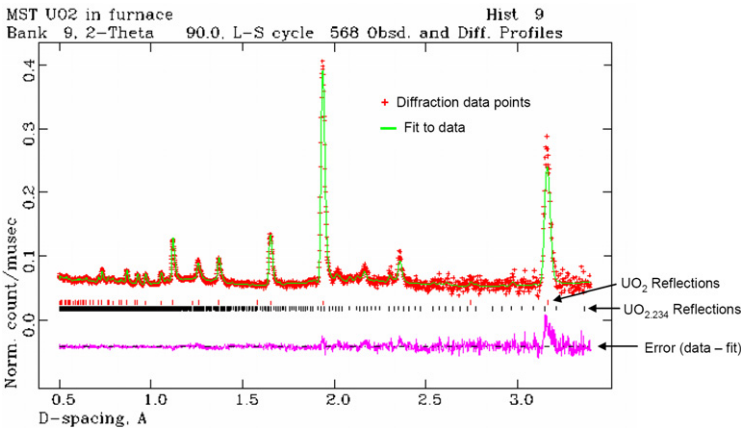

Fig. 4. Example Rietveld refinement results (taken from run 9986). Reflections shown are those considered in the refinement strategy. Note that error curve is shifted down by 0.04 units with respect to the abscissa for clarity.

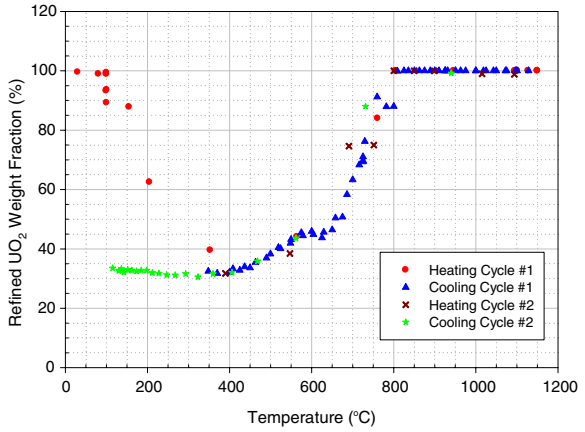

Fig. 5. Refined UO_2 phase weight fraction in sample as a function of temperature. Remaining weight fraction is $UO_{2.234}$.

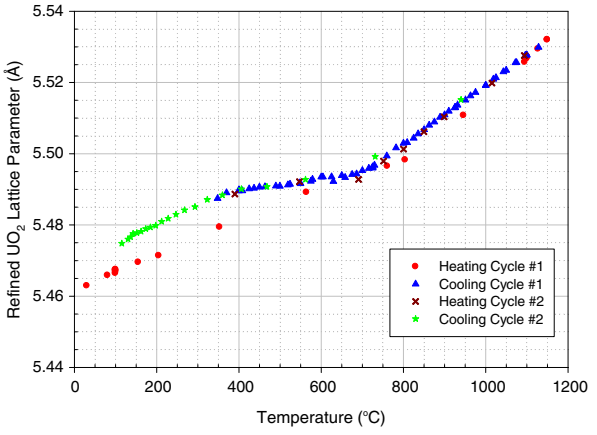

Fig. 6. Refined UO_2 phase lattice parameter.

rium, as shown by the UO_2 weight fraction dropping from ~100% to ~30% in the relatively low

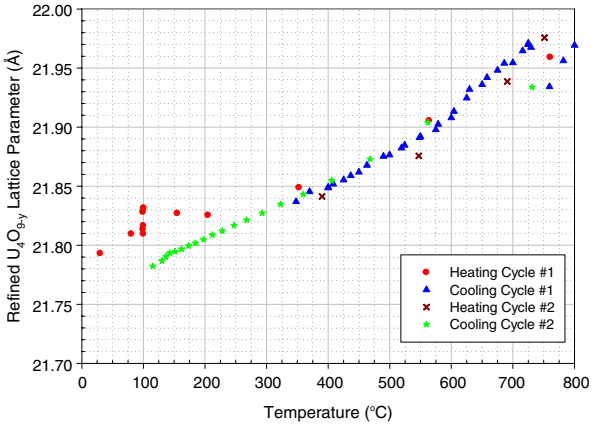

Fig. 7. Refined $UO_{2.234}$ phase lattice parameter.

100–300 °C range. Also, the high UO_2 weight fraction at low temperature could not be reproduced on either rapid (20 °C min^{-1}) or slow (<1 °C min^{-1}) cooling (compare patterns A and F in Fig. 3), suggesting that the state of the sample was permanently changed from its initial state at the beginning of the experiment. This observation agrees with previous investigators that indeed a very rapid cooling rate (i.e., quenching) is required to maintain the single phase (UO_{2+x}). As shown in Figs. 5–7, all refined parameters (weight fraction and lattice parameters) were reproducible after the initial heat up, suggesting the overall composition of the sample was not changing. Thus, it appears that the vacuum maintained in the furnace (<10^{-5} Torr) and the seal on the sample holder were sufficient to prevent any additional oxygen uptake by the sample.

The smaller lattice parameter for the UO_2 phase on initial heat up, which was not reproducible

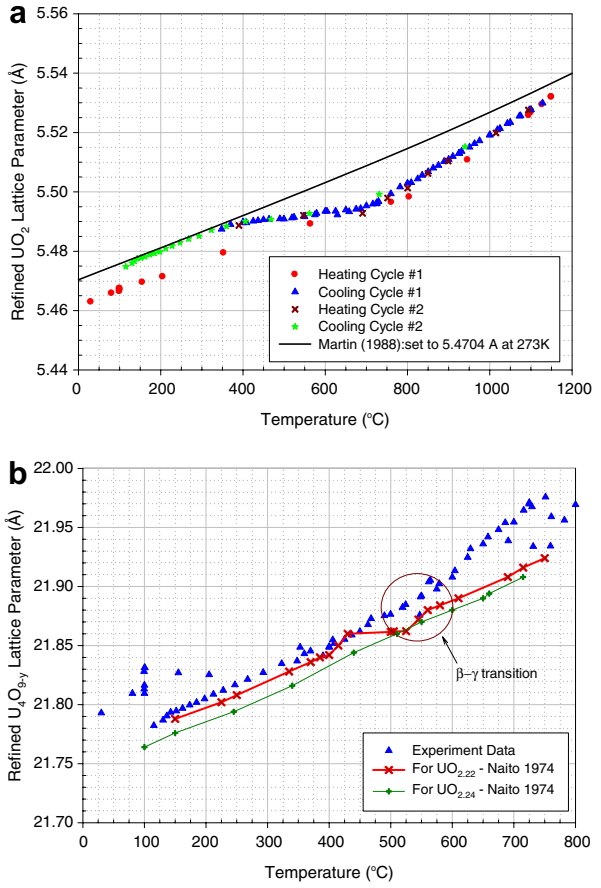

Fig. 8. Lattice parameters at various temperatures for the (a) UO_2 and (b) U_4O_{9-y} phases. Martin data taken from [31]. Naito data taken from [5].

upon reheating, is consistent with a hyperstoichiometric UO_2 phase, as the UO_{2+x} crystal shrinks with increasing x [30].

Based on the conclusion that the sample was initially a single UO_{2+x} phase, some useful information about low temperature precipitation of U_4O_{9-y} can be observed. In particular, this experiment shows, at least qualitatively, that U_4O_{9-y} can precipitate out of UO_{2+x} at relatively low temperatures. In particular, at a temperature of only 300 °C this system can approach thermodynamic phase equilibrium in a relatively short period of time (less than 1 h). This information may be useful for planning experiments on this system where annealing is required to ensure equilibrium. Modeling of low temperature behaviour of oxidized fuel may also benefit from this observation.

The values of UO_2 and $UO_{2.234}$ lattice parameters obtained from the refinement were compared with published values, as shown in Fig. 8. Note that values of U_4O_{9-y} lattice parameter above 800 °C are not shown as Fig. 5 shows that above this temperature the sample was entirely UO_{2+x}.

The refined UO_2 lattice parameters below 400 °C for the runs after the initial heat up are in excellent agreement with the lattice parameter-temperature correlation of Martin [31], however above 400 °C the experimental lattice parameter deviates from the expected linear coefficient of thermal expansion (CTE) behaviour. This apparent discrepancy can be explained by examination of the U–O phase dia-

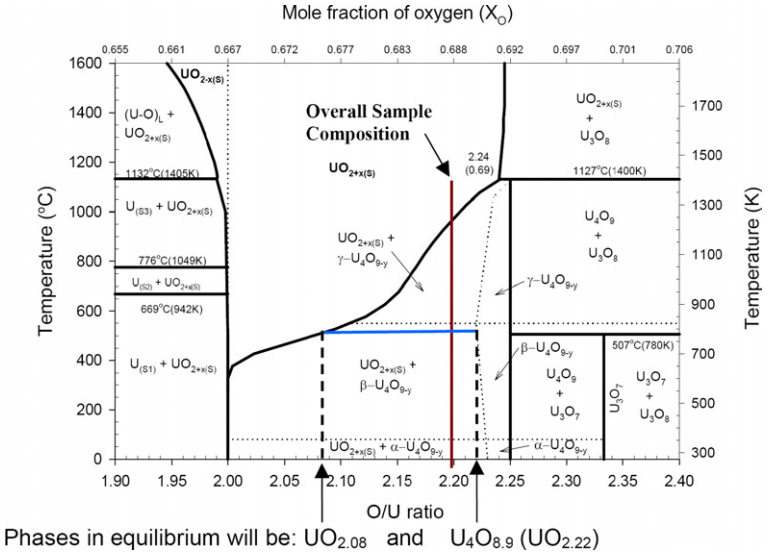

Fig. 9. Tie line construction demonstrating phases in equilibrium.

gram in this area (Fig. 9). Here it can be seen that at low temperature (below 400 °C), the composition of the UO_2 phase in the sample would be very nearly stoichiometric $UO_{2.00}$. As the temperature of the sample increases above 400 °C, however, the non-stoichiometry in the UO_2 phase will increase (the composition of the U_4O_{9-y} phase will also decrease). In this case, at 500 °C, the composition will be approximately $UO_{2.08}$ according to the phase diagram. Thus, above 400 °C, the UO_2 phase in the sample is no longer stoichiometric, but increasingly hyperstoichiometric, resulting in a decrease of the lattice parameter superposed on the thermal expansion. The UO_{2+x} lattice parameter decreases with increasing positive deviation from stoichiometry [26,29,32], but still increases with increasing temperature. Thus, a competing effect on lattice parameter exists, with the net result being a decreased slope of UO_2 lattice parameter (with temperature), as shown in Fig. 8(a). At approximately 750 °C, the slope increases and remains constant, suggesting the UO_{2+x} phase composition is no longer changing. This is consistent with the crossing of the UO_{2+x}/U_4O_{9-y} phase boundary and dissolution of any remaining U_4O_{9-y} into a single UO_{2+x} phase. This observation is confirmed with a refined UO_2 phase weight fraction of 100% above approximately 800 °C, as shown in Fig. 5.

The Martin correlation was suggested to be applicable to both $UO_{2.00}$ and UO_{2+x} for x values in the range 0–0.13 and 0.235–0.25 up to 1520 K. Therefore, it is not surprising that the slope of the UO_2 lattice parameter above 800 °C appears slightly higher than that of the Martin correlation. Data from Martin suggests that for O/U ratios near 2.20, the slope is indeed higher than the correlation, as has been observed (Fig. 8(a)).

As expected, the slope (but not actual values) of the UO_2 lattice parameter on initial heat up below 200 °C is very similar to that of Martin, suggesting its composition is not changing (as shown in a nearly constant weight fraction below 200 °C in Fig. 5). The values are shifted lower than that of Martin, however, suggesting the phase is hyperstoichiometric.

As shown in Fig. 8(b), the refined U_4O_{9-y} lattice parameter values compare well with the experimental data of Naito [5]. In particular, the agreement is slightly better when compared with $UO_{2.22}$ data as opposed to $UO_{2.24}$ data. This would suggest that the U_4O_{9-y} phase composition in the sample was close to $UO_{2.22}$. This is consistent with the phase boundary data (Fig. 1). The experimental U_4O_{9-y} lattice parameter values do appear to begin to deviate (and scatter more) from published data above 600 °C (Fig. 8(b)). There are two reasons why this may be occurring: Above 550 °C, the U_4O_{9-y} phase fraction is decreasing rapidly (Fig. 5), thus diffraction peak intensities for this phase are decreasing, making it more difficult to distinguish the phase in the refinement and thus increasing the refinement error. Alternatively, the use of the β-U_4O_{9-y} crystal structure for all temperatures for the refinement may be leading to inaccuracies at temperatures above 550 °C where the γ-U_4O_{9-y} phase predominates. Unfortunately, no crystal structure for γ-U_4O_{9-y} was found in the literature.

Data from this experiment can be used to compare with the suggested U_4O_{9-y} phase boundaries by using the lever rule with the refined UO_2 weight fractions, if the overall composition (i.e., O/U ratio) of the sample is known, as shown in Fig. 10.

Using a TGA, the batch of depleted UO_2 from which the sample came was tested at LANL. The sample was heated in an oxidizing environment and the weight gain to oxidize it to U_3O_8 was measured. From this weight gain the overall O/U of the sample was calculated to be 2.197 [33]. The authors suggest the variability in the TGA measurement to be 2.20 ± 0.03.

From Fig. 5, the U_4O_{9-y} decomposition temperature can be estimated to be 800 °C. If the sample was in fact $UO_{2.197}$, the decomposition temperature should be closer to 1000 °C (Fig. 10). The UO_{2+x}/U_4O_{9-y} phase boundary is well established by many investigators, as shown by Fig. 1 and thus a discrepancy of 200 °C due to improper placement of the phase boundary is unlikely. Also, using the lever rule (Fig. 10), at low temperature (below 400 °C) for an overall composition of $UO_{2.197}$, the UO_2 weight fraction is calculated to be approximately 14%, which is considerably lower than that determined from the refinement of the experimental data (~32% from Fig. 5). Considering these factors, as well as the stated uncertainty in the O/U measurement on this material, the overall composition of the sample is taken to be $UO_{2.17}$ to be consistent with the repeatable decomposition temperature of 800 °C.

Using an overall composition of $UO_{2.17}$ for the sample and applying the lever rule as shown in Fig. 10, the phase fractions, and thus weight fractions, of UO_{2+x} and U_4O_{9-y} can be determined from the phase diagram at various temperatures. These values are then compared with the UO_2

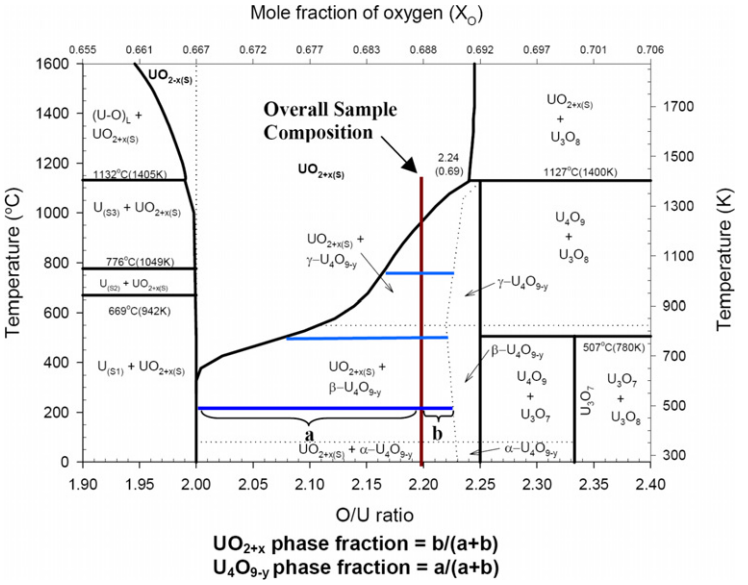

Fig. 10. Graphical representation of lever rule as applied to the U–O system.

weight fractions determined from the Rietveld refinement of the neutron diffraction patterns. This comparison is shown in Fig. 11. Overall, the general trend of the phase diagram is captured with the neutron diffraction data. There appears to be some difference in the 600–700 °C range. The data points and error bars on the figure represent temperatures where the narrow non-stoichiometry in U_4O_{9-y} has been measured, as shown in Fig. 1. Unfortunately, there appears to be only one set of measurements [18] on the location of the UO_{2+x}/U_4O_9 phase boundary in the temperature range in question (600–700 °C) and still there is no data for this boundary between 550 °C and 650 °C. Kim et al. [26], using neutron diffraction on UO_{2+x} samples at a few temperatures, also found a deviation in the refined weight fractions from that expected based on the phase diagram.

In summary, the neutron diffraction experiment has demonstrated that U_4O_9 does have a sub-stoichiometric field and that precipitation of U_4O_{9-y} from UO_{2+x} can be captured using neutron diffraction studies. It also shows that the kinetics of precipitation are indeed fast (i.e., at least as fast as the

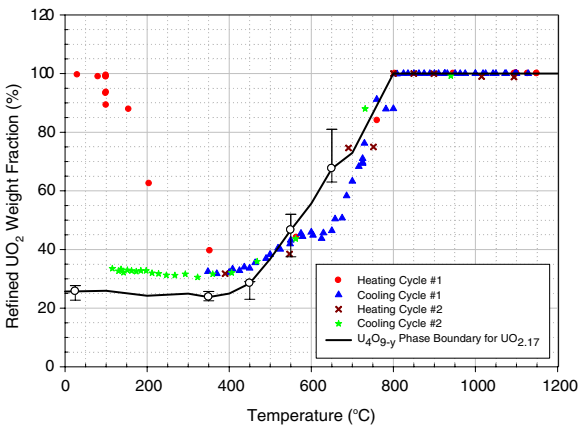

Fig. 11. Comparison of refined UO_2 weight fraction with the phase diagram of Fig. 1 based on an overall composition of $UO_{2.17}$.

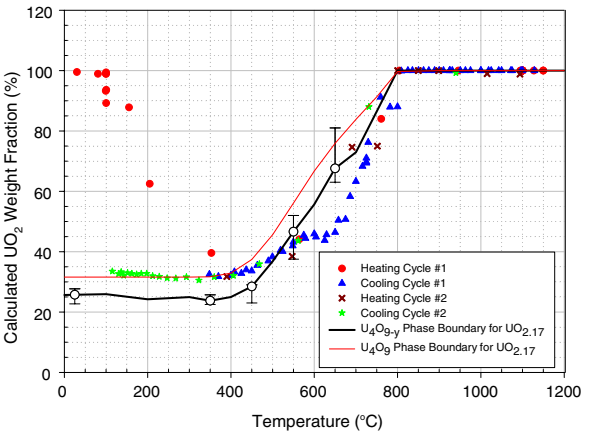

Fig. 12. Comparing refined UO_2 weight fractions with U–O phase diagram considering both stoichiometric and non-stoichiometric U_4O_9.

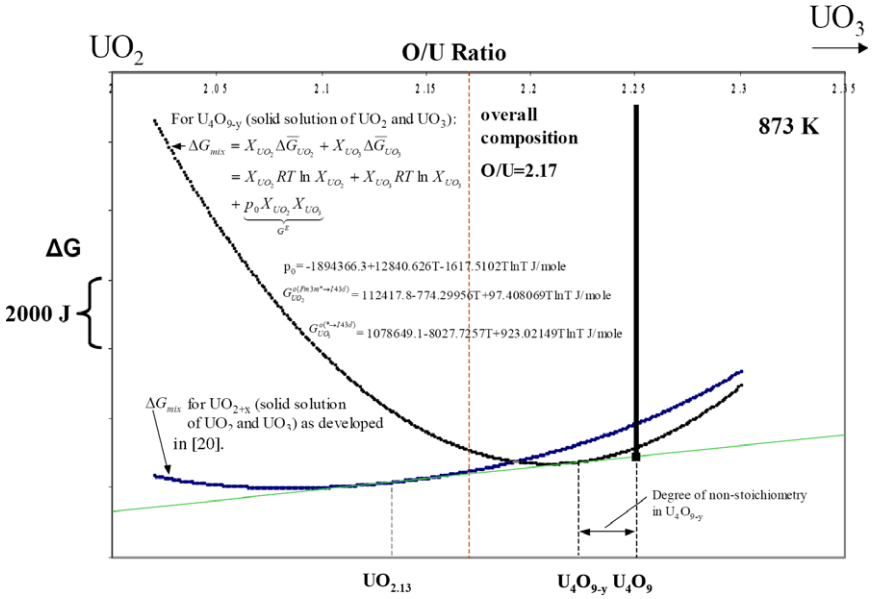

Fig. 13. Gibbs free energy curves for solid solutions of UO_2 and UO_3 representing the non-stoichiometric phases of UO_{2+x} and U_4O_{9-y}.

maximum temperature change of the apparatus used $-1200\ ^\circ C\ h^{-1}$) as the metastable UO_{2+x} phase found on initial heating could not be reproduced.

The refined UO_2 weight fractions were also compared with the calculated U–O phase diagram, assuming U_4O_9 was a stoichiometric phase, as shown in Fig. 12. Here it can be seen that above 450 °C the neutron diffraction data are in closer agreement to the non-stoichiometric U_4O_{9-y} phase, however, below 450 °C, it appears the data suggest U_4O_9 is stoichiometric. From this observation, it may be suggested that the extent of non-stoichiometry of U_4O_9 at low temperatures (below 400 °C) is negligible. This is consistent with early U–O phase diagrams, such as that by Cordfunke [34] and Cox et al. [35].

A thermodynamic treatment for U_4O_{9-y} as a non-stoichiometric phase could be developed based on the neutron diffraction data for U_4O_{9-y}. Similar to the treatment for UO_{2+x} as presented in [20], U_4O_{9-y} could also be modeled as a solid solution of UO_2 and UO_3 since UO_{2+x} and U_4O_{9-y} have a very similar crystal structure. To demonstrate the feasibility of such an endeavor, the γ- U_4O_{9-y} phase treatment was developed using a similar approach to that for UO_{2+x}. Fig. 13 shows the calculated Gibbs free energy of mixing curves at 873 K for both UO_{2+x} and U_4O_{9-y} in a system of a mixture of UO_2 and UO_3. The model parameters for the non-stoichiometric U_4O_{9-y} are also shown in this figure. This treatment could be expanded to the α and β phases of U_4O_{9-y} as well.

5. Conclusions

The excellent agreement of refined lattice parameters and weight fractions from the neutron diffraction experiment with published values has demonstrated that time-of-flight neutron diffraction can be a very useful tool for studies of the U–O system, even at high temperatures. The neutron diffraction experiment has demonstrated that, at approximately 300 °C, a powder sample of UO_{2+x} will reach thermodynamic equilibrium in less than 1 h and U_4O_{9-y} can begin to precipitate at only 100 °C. In addition, the data suggests that the sub-stoichiometry in U_4O_9 at room temperature is very low. These observations could be useful for preparation of space reactor fuel or for planning low temperature studies on this material.

Although the current study focused on the U–O system, the techniques used (neutron diffraction and thermodynamic modeling) could readily be applied to systems for other space reactor fuels, such as U–N or U–C.

Acknowledgements

The authors would like to acknowledge the helpful discussions with S. White (RMC) and

experimental support of D. Williams and O. Gourdon (LANL). The sample for this study was provided by J. Dunwoody (LANL). The work was funded in part by the National Science and Engineering Research Council of Canada (NSERC).

This work has benefited from the use of the Los Alamos Neutron Science Center at the Los Alamos National Laboratory. This facility is funded by the US Department of Energy under Contract W-7405-ENG-36.

References

[1] R.J. McEachern, P. Taylor, J. Nucl. Mater. 254 (1998) 87.
[2] C. Guéneau, M. Baichi, D. Labroche, C. Chatillon, B. Sundman, J. Nucl. Mater. 304 (2002) 161.
[3] P.-Y. Chevalier, E. Fischer, B. Cheynet, J. Nucl. Mater. 303 (2002) 1.
[4] B.J. Lewis, W.T. Thompson, F. Akbari, D.M. Thompson, C. Thurgood, J. Higgs, J. Nucl. Mater. 328 (2004) 180.
[5] K. Naito, J. Nucl. Mater. 51 (1) (1974) 126.
[6] B.E. Schaner, J. Nucl. Mater. 2 (1960) 110.
[7] L.E.J. Roberts, A.J . Walter, J. Inorg. Nucl. Chem. 22 (1961) 213.
[8] S. Aronson, J.E. Rulli, B.E. Schaner, J. Phys. Chem. 35 (4) (1961) 1382.
[9] M.J. Bannister, W.J. Buykx, J. Nucl. Mater. 55 (1974) 345.
[10] Y. Saito, J. Nucl. Mater. 51 (1974) 112.
[11] A. Nakamura, T. Fujino, J. Nucl. Mater. 149 (1987) 80.
[12] A.M. Anthony, R. Kiyoura, T. Sata, J. Nucl. Mater. 10 (1) (1963) 8.
[13] A. Kotlar, P. Gerdanian, M. Dode, J. Chim. Phys. 65 (1968) 687.
[14] P.E. Blackburn, J. Phys. Chem. 62 (8) (1958) 897.
[15] L.M. Kovba, Phase Diagram of the Uranium–Oxygen System, (Presented by Academician V.I. Spitsyn, 26 January, 1970) Translated from Doklady Akademii Nauk SSSR, vol. 194, No. 1, p. 98, September, 1970.
[16] W. Van Lierde, J. Pelsmaekers, A. Lecocq-Robert, J. Nucl. Mater. 37 (1970) 276.
[17] T.L Markin, R.J. Bones, U.K.A.E.A., Report AERE-R 4042, 1962.
[18] T. Ishii, K. Naito, K. Oshima, Solid State Commun. 8 (1970) 677.
[19] F. Grønvold, J. Inorg. Nucl. Chem. 1 (357) (1955).
[20] J.D. Higgs, B.J. Lewis, W.T. Thompson, Z. He, J. Nucl. Mater., in press, doi:10.1016/j.jnucmat.2006.12.050.
[21] H.-R. Wenk, L. Lutterotti, S. Vogel, Nucl. Instrum. and Meth. A 515 (2003) 575.
[22] S.C. Vogel, C. Hartig, L. Lutterotti, R.B. Von Dreele, H.-R. Wenk, D.J. Williams, Powder Diffr. 19 (2004) 64.
[23] H.M. Rietveld, J. Appl. Crystallogr. 2 (1969) 65.
[24] A.C. Larson, R.B. Von Dreele, General Structure Analysis System (GSAS), Los Alamos National Laboratory Report LAUR 86-748, 2004.
[25] M.T. Hutchings, J. Chemical Society, Faraday Trans. 2 (83) (1987) 1083.
[26] J.S. Kim, Y.-N. Choi, C.H. Lee, S.-H. Kim, Y.-W. Lee, J. Korean Ceram. Soc. 38 (11) (2001) 967.
[27] R.I. Cooper, B.T.M. Willis, Acta Crystallogr. A 60 (2004) 322.
[28] N. Masaki, K. Doi, Acta Crystallogr. B 28 (1972) 785.
[29] B. Belbeoch, C. Piekarski, P. Perio, Acta Crystallogr. 14 (837) (1961).
[30] IAEA, Interational Atomic Energy Agency, Thermodynamic and Transport Properties of UO_2, Tech. Report Series No. 39, 1965.
[31] D.G. Martin, J. Nucl. Mater. 152 (1988) 94.
[32] B.E. Schaner, J. Nucl. Mater. 2 (1960) 110.
[33] Private communication, J. Dunwoody to J. Higgs, 14 September 2005.
[34] E.H.P. Cordfunke, The Chemistry of Uranium Including its Applications in Nuclear Technology, Elsevier, New York, 1969.
[35] D.S. Cox, F.C. Iglesias, C.E.L. Hunt, N.A. Keller, R.D. Barrand, J.R. Mitchell, R.F. O'Connor, in: Proceedings of the Symposium of Chemical Phenomena Associated with Radioactivity Releases during Severe Nuclear Plant Accidents, NUREG/CP-0078, Anaheim, CA, 1986, pp. 2–35 to 2–49, US Nuclear Regulatory Commission.